*Eur. J. Mech., B/Fluids*, **12**, n° 3, 277-288, 1993

# The influence of an axial mean flow on the Couette-Taylor Problem

**R. RAFFAÏ * and P. LAURE ***

ABSTRACT. — This paper deals with the importance of an axial flux on the primary bifurcation of the Couette-Taylor system. Firstly, we explain to introduce a zero axial mean flow condition into the functional framework allowing us to compute numerically the amplitude equation. The new results yield excellent quantitative agreement with experimental and numerical simulation results above criticality. Secondly, we look at the influence of an additional small axial mean flow. This effect is treated as a perturbation to the classical situation. At small Reynolds number, this imperfection induces a Poiseuille flow in the axial direction. On increasing the Reynolds number, the transition to the stationary Taylor vortex is replaced by the appearance of a travelling wave with a group velocity two orders of magnitude larger than the Poiseuille velocity. In the case when the oscillatory non-axisymmetric modes are the most unstable, the standing waves are now quasiperiodic and the two travelling waves have slightly different frequencies and are non symmetric. Moreover, the primary stable solution which bifurcates from the Couette flow is always the travelling wave moving within the Poiseuille flow, and there are parameter ranges where the wave which travels in the opposite direction to the main flux may be stable together with the other wave. The quasiperiodic solution can occur via a secondary bifurcation as the Reynolds number increases.

## 1. Introduction

The Couette-Taylor problem is a classical illustration of the bifurcations in a system possessing SO(2) symmetry (rotations about the $z$-axis) commuting with O(2) symmetry (translation along the $z$-axis where the solution is assumed periodic in $z$ and reflection $S: z \rightarrow -z$). The parameters of the problem are the ratio of outer and inner angular velocities $\Omega = \Omega_2/\Omega_1$, the ratio of inner and outer radii $\eta = R_1/R_2$ and the Reynolds number $\Re e = R_1 \Omega_1 (R_2 - R_1)/\nu$. The final parameter, the height $h$ of the two cylinders, is usually not considered in the theoretical literature, as we assume that the cylinders are long enough to allow us to neglect the influence of boundary condition at the extremities. The two boundary conditions on the top and bottom of cylinders are replaced by an $h$-periodicity condition.

In this paper we look at the influence of an imposed small axial mean flow $\varepsilon$. This effect is discussed as a perturbation to the primary bifurcations which lead to Taylor vortices, spirals or ribbons [Chossat & Iooss, 1985]. Our work was suggested by Edwards

* Institut Non Linéaire de Nice, U.M.R.-C.N.R.S. n° 129, Université de Nice, 06108 Nice Cedex 2, France.


0997-7546/93/03 277 12/$ 3.20/ 

*et al*'s paper [Edwards *et al.*, 1991] which deals with the evolution of a spiral solution after the critical point. They point out discrepancies between nonlinear analysis [Demay & Iooss, 1984] and their experimental and numerical results. Moreover, they show that a zero axial mean flow condition has to be taken into account in order to obtain good agreement with experimental results, replacing the periodicity condition on the pressure used in [D & I, 1984].

As shown in [Chandrasekhar, 1961], the basic flow $V_b$ at small Reynolds number is now the sum of a Couette flow $V_c=(0, v_c(r), 0)$ in the azimuthal direction and a Poiseuille flow $V_p=(0, 0, v_p(r))$ in the axial direction,

$$\text{(1)}\quad V_b=(0, v_c(r), \varepsilon v_p(r)), \qquad v_c(r)=A_c r+B_c/r, \qquad v_p(r)=A_p(r^2+B_p\log(r)+C_p)$$

where all the constants are determined by the following boundary conditions

$$\text{(2)}\quad \left\{ \begin{array}{ll} 2\pi\int_{(\eta/(1-\eta))}^{(1/(1-\eta))} r v_p(r)\, r\, dr=1; & v_p\left(\frac{\eta}{1-\eta}\right)=v_p\left(\frac{1}{1-\eta}\right)=0 \\ v_c\left(\frac{\eta}{1-\eta}\right)=1; & v_c\left(\frac{1}{1-\eta}\right)=\frac{\Omega}{\eta}. \end{array}\right.$$

They yield

$$A_c=\frac{\Omega-\eta^2}{\eta(1+\eta)}; \qquad B_c=\frac{\eta(1-\Omega)}{(1-\eta)(1-\eta^2)};$$

$$A_p=\frac{2}{\pi}\frac{(\eta-1)^3\log(\eta)}{(1+\eta)[(1+\log(\eta)+\eta^2(\log(\eta)-1)]}; \qquad B_p=\frac{1+\eta}{(1-\eta)\log(\eta)};$$

$$C_p=\frac{(1-\eta^2)\log(1-\eta)-\log(\eta)}{(\eta-1)^2\log(\eta)}$$

The above solutions and the numerical results given below are scaled by the factors $R_2-R_1$, $R_1\Omega_1$, $(R_2-R_1)^2/\nu)$ for length, velocity and time respectively. We remark that the perturbation equation of this basic flow is also invariant under $O(2)\times SO(2)$ group symmetry if we incorporate $\varepsilon$ into the set of variables. The reflection S is simply replaced by the reflection $S': z\to -z;\ \varepsilon\to-\varepsilon$.

## 2. The perturbation equation and the functional set-up

The equation satisfied by the perturbation U to the basic flow $V_b$ may be put into the form of a differential equation lying in a suitable function space H

$$\text{(3)}\quad \frac{dU}{dt}=L_\mu U+\varepsilon N_\mu(V_p, U)+N_\mu(U, U) \qquad \text{where} \quad \mu=\Re-\Re_c.$$

In this formal equation, $L_\mu$ and $N_\mu$ are respectively linear and quadratic operators which depend smoothly on the parameter $\mu$, and $\Re_c$ is the Reynolds number for which the

Couette flow becomes unstable for $\varepsilon=0$. These operators are sufficently smooth to allow the application of methods of bifurcation and weakly nonlinear analysis to (3) (*see* [C & I, 1985]). The functional space H is defined by,

$$\text{(4)} \qquad \mathrm{H}=\left\{ \mathrm{U}\in[\mathrm{L}^2(\mathrm{Q}_h)]^3, \nabla.\mathrm{U}=0; \mathrm{U}.n\big|_{\partial\Sigma\times \mathrm{I}_h}=0 \text{ and } \int_\Sigma \mathrm{U}.n\,ds=0\right\}$$

where $\mathrm{Q}_h=\Sigma\times\mathrm{I}_h$ is the domain of periodicity between two concentric cylinders, $\Sigma$ the cross section $\mathrm{I}_h$ the interval $[-h/2, h/2]$ and $\mathrm{L}^2(\mathrm{Q}_h)$ the closure with respect to the norm $\mathrm{L}^2$ of the set of continuous and $h$-periodic functions of $z$ on $\mathrm{Q}_h$. The main interest in this space contains functions satisfying some of the boundary conditions and the divergence free condition, lies in the fact that the pressure is eliminated when the Navier-Stokes equation is projected on to H. We use the general decomposition for any $\mathrm{V}\in[\mathrm{L}^2(\mathrm{Q}_h)]^3$

$$\text{(5)} \qquad \begin{cases} \mathrm{V}=\mathrm{U}+\nabla\phi \qquad \text{with} \quad \mathrm{U}\in\mathrm{H}, \\ \phi=\phi'=az \text{ and } \phi' \text{ } h\text{-periodic and of square integrable first derivative on } \mathrm{Q}_h. \end{cases}$$

$a$ is a constant given by the relation

$$\text{(6)} \qquad a\Sigma=\int_\Sigma \mathrm{V}.n\,ds-\int_\Sigma \frac{d\phi'}{dn}\,ds.$$

This decomposition is an orthogonal decomposition in $[\mathrm{L}^2(\mathrm{Q}_h)]^n$. The domain of definition $(\mathscr{D})$ of U (which is $\subset\mathrm{H}$) is defined by

$$\mathscr{D}=\mathrm{H}_2(\mathrm{Q}_h)\cap\left\{\mathrm{U}\in\mathrm{H}, \mathrm{U}\big|_{\partial\Sigma\times\mathrm{I}_h}=0\right\}$$

We remark that the space H is slightly different from the one previously used by Demay and Iooss [D & I, 1984]. Demay and Iooss did not impose explicitly that the axial mean flow of the perturbation is zero. In their paper, they also consider infinite cylinders by using the usual assumption that the influence of the rigid walls (which leads to Eckman rolls) is confined to the neighborhood of boundaries. In this way, they replace the rigid boundary conditions at the two end walls by a periodicity condition on both the velocity and the pressure fields. But due to the divergence free condition, the axial mean flow of the perturbation $\left(\int_\Sigma \mathrm{U}.n\,ds\right)$ is invariant along the $z$-axis and would be equal to zero (the axial flux imposed by experimentalists is already carried by the Poiseuille velocity). Unfortunately, the constraint that the velocity field has a fixed axial mean flow, is not in general compatible with a periodic pressure. As already noted by [E *et al.*, 1991], this is true in particular for spirals as they are not invariant under S symmetry. With our new functional framework, it now possible to choose the mean pressure gradient such that the axial mean flow is zero. In practice, as we assume that the pressure gradient is periodic, the pressure $p$ will be split into two terms : $p=p'+az$ where $p'$ is z-periodic. The constant $a$ will be determined by means of a relation such as Eq. (6) in order to balance the axial flux due to the mean flow of the perturbation.

The linear analysis for $\varepsilon=0$ is the same as in previous works. We look for eigenmodes of the form $U(r, \theta, z)=\hat{U}(r)\, e^{i(\alpha z+m\theta)}$ where $\alpha$, $m$ are respectively the axial and azimuthal wavenumbers, and in the main there are two possibilities; either the critical eigenvalue is null with an azimuthal wave number $m$ equal to 0, or the critical eigenvalues are purely imaginary ($\pm i\omega$) with $m>0$.

## 3. The weakly nonlinear analysis

We use the center manifold theorem (*see* for instance [Vanderbauwhede & Iooss, 1992]) in the neighborhood of $(U, \mu, \varepsilon)=(0, 0, 0)$. The theorical information on such an imperfection can be found in [Van, 1984]. Thus, the perturbation U is split into two parts

$$U=X+\Phi(\mu, \varepsilon, X), \qquad \Phi(\mu, \varepsilon, 0)=0 \quad \text{and} \quad \frac{\partial \Phi}{\partial X}(0, 0, 0)=0 \tag{7}$$

where X belongs to the eigenspace generated by the critical modes of $L_0$ and $\Phi$ belongs to the complementary space. The amplitude equation is obtained by the projection of Eq. (3) into the critical subspace of $L_0$ for the perturbation U belonging to the center manifold [Eq. (7)]. As the symmetry properties are satisfied by this reduced system, we can deduce the form of its Taylor expansion. Consequently, the new amplitude equation, in the non-oscillatory case, reads

$$X=AU_0+\bar{A}\bar{U}_0; \qquad \frac{dA}{dt}=A(a\mu+b|A|^2+\mathrm{i}d\,\varepsilon+e\,\varepsilon^2)+\ldots \tag{8}$$

where the critical mode $U_0=\hat{U}_0(r)\, e^{i(\alpha z)}$ is axisymmetric and the coefficients $a$, $b$, $d$, $e$ are real.

In the oscillatory case, we obtain, in the same way, the following system

$$X=AU_1+BS(U_1)+cc; \tag{9}$$
$$\begin{cases} d_t A=A(i\omega_c+a\mu+b|A|^2+c|B|^2+d\varepsilon)+\ldots \\ d_t B=(i\omega_c+a\mu+b|B|^2+c|A|^2-d\varepsilon)+\ldots \end{cases}$$

where the critical mode $U_1=\hat{U}_1(r)\, e^{i(\alpha z+m\theta)}$. The numerical method used to give these coefficients is similar to the one used in [D & I, 1984] (*see* also [Raffai, 1992] for all the details) and they are computed with the critical mode normalized such that $\hat{U}_i((1+\eta)/2(1-\eta))=1$, $i=0$ or 1.

In Table I, numerical values of coefficients in Eq. (9) are presented for the same parameter values as [D & I, 1984].

### 3.1. The case of zero mean flow ($\varepsilon = 0$)

We now compare our nonlinear coefficients with those computed by [D & I, 1984]. In the stationary case, due to the symmetry S the zero mean flow condition is automatically satisfied and the values of coefficients $a$ and $b$ in (8) are the same as those computed by [D & I, 1984].

Eq. (9) possesses two types of non trivial solutions, travelling waves ("spirals") ($A \neq 0$ and $B = 0$, or the contrary) and standing waves (ribbons) ($|A| = |B|$). The former is stable with respect to homogeneous perturbations when $b_r < 0$ and $c_r - b_r < 0$, the latter when $b_r - c_r < 0$ and $c_r + b_r < 0$ (the subscripts "$r$" and "$i$" mean respectively the real part and the imaginary part). Thus, two areas of stability are defined in the plane ($b_r$, $c_r$) [C & I, 1985] and the real part of coefficients $b$ and $c$ belong to these domains or otherwise according to the values of the two parameters $\eta$ and $\Omega$. The new numerical values are different from the previous ones [D & I, 1984]. But, the domain of stability of spirals or ribbons with respect to the velocity ratio $\Omega$ is the same for the two values of the radius ratio $\eta = .7519$ and $.95$. However, we show below that the null mean flow condition allows us to obtain better agreement with experimental and numerical results, far from criticality. The behavior of the bifurcated solutions is described by the amplitude Eq. (9) expanded to fifth order because the third order terms give only the slope at the critical point of the curve giving the frequency as a function of $\mu$. The amplitude equation satisfied by the spiral ($A \neq 0$ and $B = 0$) is

$$\frac{dA}{dt} = A\,(i\omega_c + a\mu + b\,|A|^2 + f\,|A|^4 + g\mu\,|A|^2 + h\mu^2 + \ldots) \tag{10}$$

The higher order coefficients $f$, $g$ and $h$ are computed with the program presented in [Laure & Demay, 1988]. If we write $A = \rho\, e^{i\omega t}$ we obtain

$$\begin{cases} 0 = f_r \rho^4 + (b_r + g_r \mu)\,\rho^2 + (a_r \mu + h_r \mu^2), \\ \omega = \omega_c + a_i \mu + h_i \mu^2 + (b_i + g_i \mu)\,\rho^2 + f_i \rho^4 \end{cases} \tag{11}$$

The evolution of the frequency $\omega$ with Reynolds number $\mathfrak{R}$ is plotted in Figure 1 for $\eta = .7992$, $\Omega = -0.74$, $m = 2$ and $\alpha = 3.6997$. The frequency $\omega$ is scaled with the inner cylinder angular velocity $\Omega_1 = \Omega_{1c}\,(1 + (\mu/\mathfrak{R}_c))$ in order to remove experimental uncertainty in viscosity. The previous results [D & I, 1984] and [E *et al.*, 1991] are also plotted and we observe that the line at critical point given by third order terms has to be corrected by the fifth order terms, which allows to agree with the numerical and experimental results with an accuracy of 2%.

### 3.2. The stationary bifurcation when $\varepsilon \neq 0$

We show that the bifurcation now takes place for $\mathfrak{R} = \mathfrak{R}_c - (e/a)\,\varepsilon^2$. Thus, the flux produces a small shift of critical Reynolds number, and the amplitude A varies in time

TABLE I. — Numerical values of coefficients in Eq. (9). They are presented with the scaling factors $R_2 - R_1$, $R_1 \Omega_1$, $(R_2 - R_1)^2/\nu$ for length, velocity and time.

| $\eta$ | $\Omega$ | $\Re_c$ | $m$ | $\alpha$ | $\omega_c$ | $a$ | $b$ | $c$ | $d$ |
|---|---|---|---|---|---|---|---|---|---|
| .95 | −0.73 | 251.09 | 1 | 3.42 | −4.76 | .130 − .024 $i$ | 15.51 + 35.84 $i$ | −54.58 − 42.74 $i$ | .116 − 8.167 $i$ |
| | −0.76 | 257.96 | 1 | 3.52 | 4.99 | .131 − .024 $i$ | 27.37 + 38.71 $i$ | −45.53 − 45.77 $i$ | .125 − 8.495 $i$ |
| | | 257.86 | 2 | 3.51 | −9.81 | .131 − .047 $i$ | 8.32 + 69.63 $i$ | −58.45 − 89.26 $i$ | .230 − 8.442 $i$ |
| | −0.80 | 266.53 | 2 | 3.57 | −10.37 | .132 − .047 $i$ | 22.85 + 75.98 $i$ | −42.53 − 98.17 $i$ | .243 − 8.821 $i$ |
| | | 266.37 | 3 | 3.56 | −15.10 | .131 − .068 $i$ | −4.42 + 95.88 $i$ | −68.12 − 141.20 $i$ | .326 − 8.755 $i$ |
| | −0.88 | 282.31 | 3 | 3.63 | −16.51 | .131 − .067 $i$ | 22.12 + 113.57 $i$ | −26.80 − 171.34 $i$ | .340 − 9.357 $i$ |
| | | 282.18 | 4 | 3.63 | −21.06 | .129 − .087 $i$ | −11.08 + 121.40 $i$ | −78.07 − 216.0 $i$ | .411 − 9.331 $i$ |
| | −1.04 | 321.76 | 4 | 3.70 | −24.22 | .126 − .085 $i$ | 41.18 + 169.62 $i$ | 22.78 − 324.79 $i$ | .397 − 10.310 $i$ |
| .7519 | −.6 | 120.92 | 1 | 3.62 | −13.70 | .300 − .133 $i$ | −89.41 + 111.30 $i$ | −205.09 − 116.24 $i$ | .841 − 22.38 $i$ |
| | −.7 | 134.29 | 1 | 3.83 | −16.28 | .308 − .128 $i$ | −49.56 + 145.87 $i$ | −168.09 − 183.70 $i$ | .856 − 25.72 $i$ |
| | | 134.28 | 2 | 3.76 | −28.82 | .284 − .249 $i$ | −151.05 + 201.18 $i$ | −301.99 − 269.99 $i$ | 1.500 − 25.30 $i$ |
| | −1.06 | 180.34 | 2 | 3.88 | −42.88 | .258 − .241 $i$ | −57.50 + 543.53 $i$ | 196.86 − 1510.6 $i$ | 1.016 − 33.14 $i$ |
| | −.38 | 94.37 | 1 | 3.80 | −26.45 | .413 − .325 $i$ | −477.22 + 294.27 $i$ | −817.16 − 103.80 $i$ | 2.92 − 43.00 $i$ |
| .5 | −.4 | 96.80 | 1 | 3.83 | −27.56 | .414 − .324 $i$ | −487.00 + 310.53 $i$ | −829.1 − 150.08 $i$ | 2.96 − 44.22 $i$ |
| | −.5 | 111.31 | 1 | 4.074 | −34.41 | .424 − .321 $i$ | −596.63 + 479.19 $i$ | −967.95 − 539.20 $i$ | 2.88 − 52.25 $i$ |

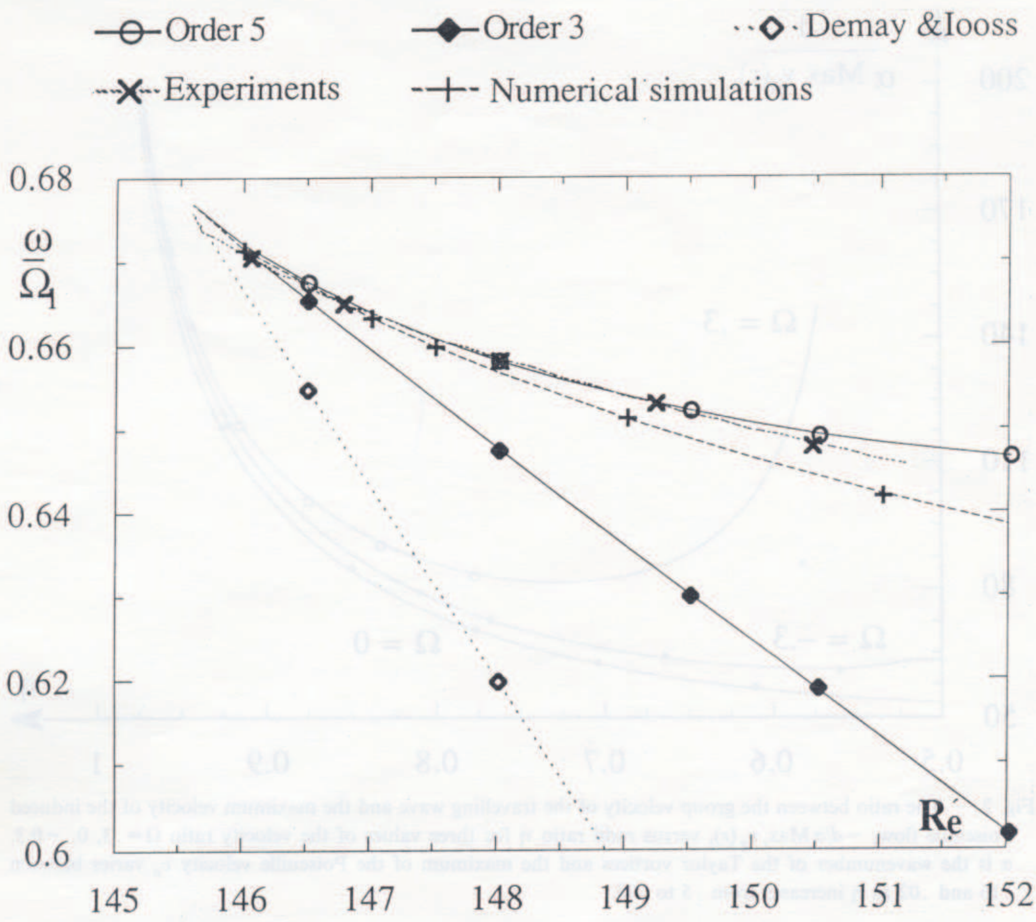


Fig. 1. − The frequency of spiral vortices versus Reynolds number. The values of the parameters are $\eta=0.7992$, $\Omega=-.74$, $m=2$, $\alpha=3.6997$, $\Re_c=145.57$ and $\Omega_{1c}=36.5778$.

with frequency $d\varepsilon$. An approximate solution of the Navier-Stokes equations is

$$V=V_c(r)+\varepsilon V_p(r)+\rho \hat{U}_0(r)e^{i(\alpha z+\omega dt)}+cc+\dots \tag{12}$$

with $\rho^2=-(b/a)\mu-(e\varepsilon^2/a)$. Numerical computations of the coefficients $d$ and $e$ are made for the three velocity ratios $\Omega=0$, 0.3, −0.3 and $\eta$ in the range .5 and .98. As the coefficients $d$ and $e$ are always negative and positive respectively, a mean flow $\varepsilon$ in the axial direction induces an advanced bifurcation towards travelling waves moving in the same direction as the Poiseuille flow, $\varepsilon V_p$. Moreover, we point out that the group velocity, $-(d/\alpha)\varepsilon$ of the travelling wave is two orders of magnitude larger than the maximum of the Poiseuille velocity. This is illustrated in Figure 2 where the evolution of ratio $-(d/\mathrm{Max}_r v_p(r)\alpha)$ with $\eta$ is plotted.

We remark that the coefficient $d$ is simply the derivative with respect to $\varepsilon$ of the critical eigenvalue at point $(\mu, \varepsilon)=(0, 0)$. Therefore, its sign is confirmed by the experimental results reported in [C, 1961]. The second coefficient $e$ has been checked by comparison

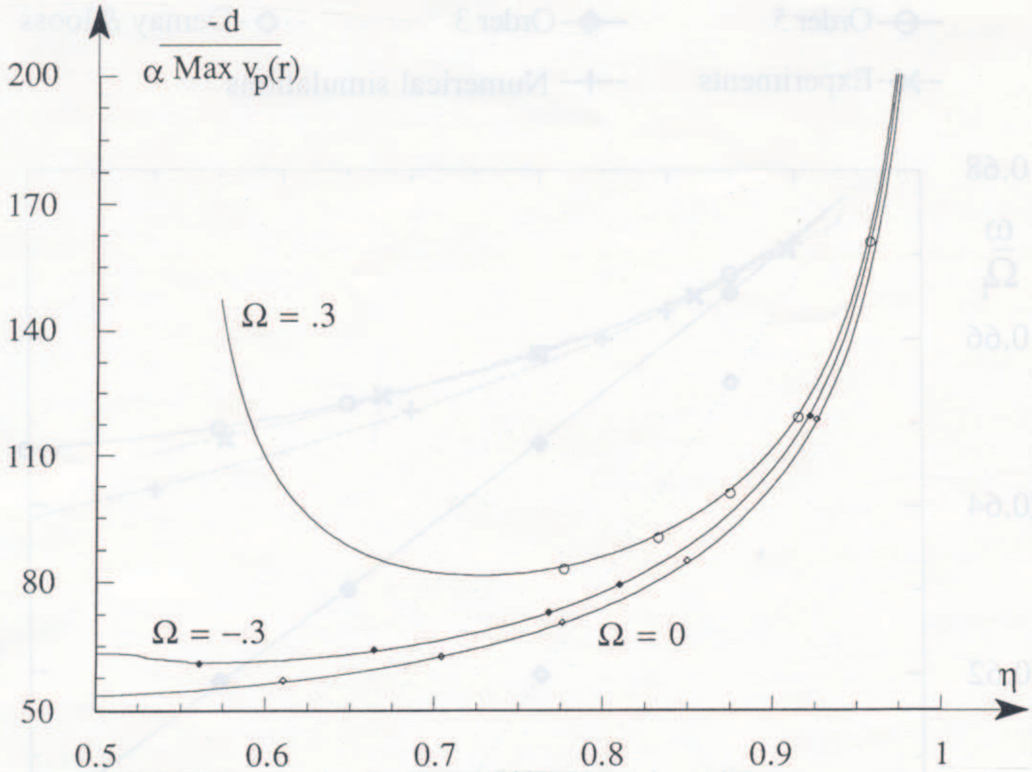


Fig. 2. − The ratio between the group velocity of the travelling wave and the maximum velocity of the induced Poiseuille flow, $-d/\alpha \,\mathrm{Max}_r v_p(r)$, versus radii ratio η for three values of the velocity ratio $\Omega = .3,\ 0,\ -0.3$. α is the wavenumber of the Taylor vortices and the maximum of the Poiseuille velocity $v_p$ varies between .16 and .02 as η increases from .5 to .98.

with experimental formulae connecting the axial mean flow and the critical Reynolds number obtained in [B *et al.*, 1991] for $\Omega=0$ and $\eta=.738$. There is a rather good agreement with the first term of their relation which expresses the quadratic dependence of the critical Reynolds on ε (we obtain .5228 instead of .5213 in [B *et al.*, 1991]).

### 3.3. The oscillatory instability when $\varepsilon \neq 0$

If the mean flow is different from zero ($\varepsilon \neq 0$), the simplest solutions of system (9) are the two travelling waves, $S^+$ ($A \neq 0$; $B=0$) and $S^-$ ($A=0$; $B \neq 0$), and a quasiperiodic solution ($|A| \neq |B|$ and non zero). Recall that the travelling waves $S^+$ and $S^-$ have positive and negative phase velocities in the *z*-direction respectively (as shown on Table I, $\omega_c$ is negative whereas α is positive). The critical Reynolds number of each solution varies linearly with ε from the non-perturbed value. The sign of the shift is given by the coefficient $d_r$. The values of $d_r$ presented in the Table I for various values of *m*, η and Ω show that this coefficient is always positive.

We write $A=\rho_+ e^{i\omega_+ t}$, $B=\rho_- e^{i\omega_- t}$, and obtain for each solution

$$S^+(\rho_+, 0)\left\{\begin{array}{l}\rho_+^2=-\dfrac{a_r}{b_r}\mu-\dfrac{d_r}{b_r}\varepsilon\\[2mm] \omega_+=\omega_c+\dfrac{a_i b_r-b_i a_r}{b_r}\mu-\dfrac{d_r b_i-d_i b_r}{b_r}\varepsilon.\end{array}\right.$$

$$S^-(0, \rho_-)\left\{\begin{array}{l}\rho_-^2=-\dfrac{a_r}{b_r}\mu+\dfrac{d_r}{b_r}\varepsilon\\[2mm] \omega_-=\omega_c+\dfrac{a_i b_r-b_i a_r}{b_r}\mu+\dfrac{d_r b_i-d_i b_r}{b_r}\varepsilon.\end{array}\right.$$

$$QP(\rho_+, \rho_-)\left\{\begin{array}{l}\rho_+^2=-\dfrac{a_r}{b_r+c_r}\mu-\dfrac{d_r}{b_r-c_r}\varepsilon\\[2mm] \rho_-^2=-\dfrac{a_r}{b_r+c_r}\mu+\dfrac{d_r}{b_r-c_r}\varepsilon\\[2mm] \omega_++\omega_-=2\omega_c+2\left(a_i-a_r\dfrac{b_i-c_i}{b_r+c_r}\right)\mu\\[2mm] \omega_+-\omega_-=2d_r\left(1-\dfrac{b_i-c_i}{b_r+c_r}\right)\varepsilon\end{array}\right.$$

A stability analysis of equations (9) for these solutions leads to the following stability conditions

(13) $\qquad b_r<0 \quad$ and $\quad k_1\mu-k_2\varepsilon>0 \quad$ for $S^+$

(14) $\qquad b_r<0 \quad$ and $\quad k_1\mu+k_2\varepsilon>0 \quad$ for $S^-$

(15) $\qquad (b_r-c_r)<0 \quad$ and $\quad (b_r+c_r)<0 \quad$ for QP

where $k_1=(b_r-c_r)$ and $k_2=d_r/a_r(b_r+c_r)$.

Therefore, we recover the condition $b_r<0$ for the travelling waves and the stability conditions for the quasiperiodic solution QP are the same as those for the ribbons when $\varepsilon=0$. Moreover, the two lines

$$D_1: k_1\mu-k_2\varepsilon=0, \qquad D_2: k_1\mu+k_2\varepsilon=0$$

which bound the domain of stability in the $(\varepsilon, \mu)$ plane for the travelling waves also delimit the area of existence of the quasiperiodic solution. Finally, the domain of existence for the two travelling waves $S^+$ and $S^-$ are given respectively by the region between the two following lines (depending on the sign of $b_r$)

$$d_1: \mu+\frac{d_r}{a_r}\varepsilon=0, \qquad d_2: \mu-\frac{d_r}{a_r}\varepsilon=0$$

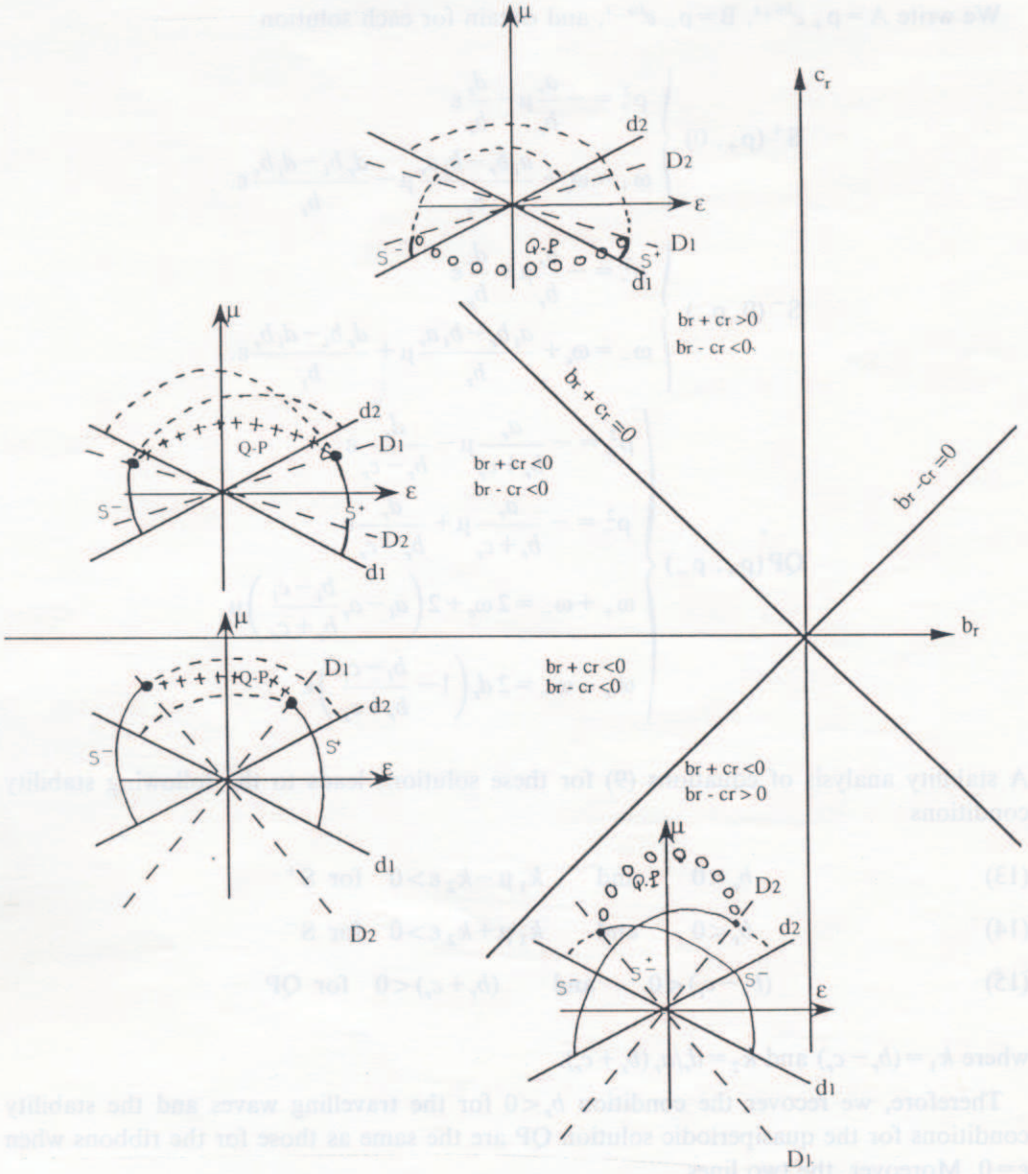

Fig. 3. − The existence and stability domains for the two travelling waves $S^+$, $S^-$ and the quasiperiodic solution QP (*see* Eq. (9) and paragraph (3.3)). Solid and dotted lines give respectively the regions of stability and the instability of solutions $S^+$ and $S^-$, whereas the plus signs + and circles ∘ correspond respectively to domain of existence of stable and unstable quasiperiodic solution QP.

Figure 3 allows us to explain the influence of a small axial flux on the existence and stability of these three solutions. In this $(b_r, c_r)$ plane, we have as in the usual case, mainly to consider three regions. (When $b_r > 0$, the solutions, if they exist, are always unstable.) One notices that in the other case ($b_r < 0$), there is always a transition from

Couette flow to travelling waves for a smaller Reynolds number than for the non perturbed case ($\varepsilon=0$) (the new $\mu_c$ is negative).

The first region ($b_r<0$ and $b_r-c_r>0$) corresponds to the case where at at $\varepsilon=0$ the two travelling waves $S^+$ and $S^-$ are stable and the standing wave exists but it is unstable. The quasiperiodic solution QP remains unstable, but the two travelling waves $S^+$ and $S^-$ have two different areas of stability in the ($\varepsilon$, $\mu$) plane. Then, if one increases the axial mean flux $\varepsilon$ at a fixed Reynolds number $\mu$, these two solutions can coexist. Whereas for higher values of $\varepsilon$ only the travelling wave moving in the same direction as the flux selected, the other one becomes unstable. In the same way, when the Reynolds number increases at fixed axial mean flux, we observe the transition from the Couette flow to the travelling wave moving in the flux's direction.

In the second region ($b_r+c_r<0$ and $b_r-c_r<0$), there exist three distinct areas in the ($\varepsilon$, $\mu$) parameter plane where these three solutions exist and are stable. However, the travelling wave moving in the flux direction is always the first bifurcated solution and the quasiperiodic solution corresponds to a secondary bifurcation as the Reynolds number increases.

In the third region ($b_r+c_r>0$ and $b_r-c_r<0$), the two travelling waves are observed for a small range of specified values of $\varepsilon$ and $\mu$, but they always become unstable as we increase the Reynolds number. The quasiperiodic solution can exist but it is unstable.

## 4. Conclusion

The addition of the null mean flow condition into the weakly nonlinear analysis improves the qualitative agreement with experimental and numerical results far from criticality. The effect of a small axial flux is also studied as perturbation. This induces at small Reynolds number an axial Poiseuille flow and as the reflection symmetry S is broken, the bifurcated solutions are no longer invariant under this symmetry. In fact, by increasing the Reynolds number at a fixed axial flux $\varepsilon$, we have, in general, an advanced bifurcation to a travelling wave moving in the same direction as the Poiseuille flow. More precisely, in the case where the most unstable modes are stationary, the Taylor rolls are replaced by a travelling wave with a group velocity proportional to $\varepsilon$. In the other case where the critical modes are oscillatory, higher Reynolds numbers one in the domain of stability of the opposite non symmetric travelling wave or a quasiperiodic. The two non-symmetric travelling waves are both stable in the parameter range where travelling waves are stable for $\varepsilon=0$. On the other hand, the quasiperiodic solution QP occurs as a secondary bifurcation in the parameter range where the standing waves are stable for $\varepsilon=0$.

## Acknowledgments

The authors would like to thanks G. Iooss, Y. Demay for fruitful comments on the subject and W. S. Edwards for having communicated to us the numerical results given in Figure 1.

## REFERENCES

BABCOCK K. L., CANNELL D. S., AHLERS G., 1991, Stability and Noise in Taylor-Couette Flow with Through-Flow, *Physica D* (to appear).

S. CHANDRASEKHAN, 1961, Hydrodynamic and Hydromagnetic Stability, Oxford University Press.

CHOSSAT P., IOOSS G., 1992, *The Couette-Taylor problem* (book in preparation).

CHOSSAT P., IOOSS G., 1985, Primary and Secondary Bifurcation in the Couette-Taylor problem, *Jap. J. Appl. Math.*, *2*, 37-68.

DEMAY Y., IOOSS G., 1984, Calcul de solutions bifurquées pour le problème de Couette-Taylor avec les deux cylindres en rotation, *J. Méca. Théo. Appl.*, numéro spécial 1984, 193-216.

EDWARDS W. S., TAGG R. P., DORNBLASER B. C., TUCKERMAN L. S., SWINNEY H. L., 1991, Periodic Traveling Waves with Nonperiodic Pressure, *Eur. J. Mech. B/Fluids*, *10*, n° 2-Suppl., 205-210.

LAURE P., DEMAY Y., 1988, Symbolic computation and equation on the center manifold, *Computers and Fluids*, *16*, 229.

RAFFAÏ R., 1993, *Thesis*, University of Nice.

VANDERBAUWHEDE A., IOOSS G., 1992, Center Manifol Theory in Infinite Dimensions, *Dynamics reported*, New series I, 125-163.

S. A. VAN GILS, 1984, *Some studies in Dynamical System theory*.

(Manuscript received June 30, 1992;
accepted August 20, 1992.)